International Journal of
Science and Engineering Investigations vol. 6, issue 67, August 2017
ISSN: 2251-8843

# Laboratory Study of Turbulence Intensity in Longitudinal, Transverse and Deep Directions and Turbulent Burst Event around Various L-Shaped Groynes

Fatemeh Veisi[1], Ahmad Jafari[2]
[1]MSc Student, Department of Water Engineering, Ramin Agriculture and Natural Resources University of Khuzestan, Iran
[2]Department of Water Engineering, Ramin Agriculture and Natural Resources University of Khuzestan, Iran
([2]jafary_ahmad@yahoo.com)

***Abstract***- Groyne structure has been used for indirect coastal protection that has a simple structure and low execution cost. Flow field around the groyne is very complex. The purpose of present research is to study turbulence intensity in longitudinal, transverse and deep directions and turbulent burst phenomenon around various L- shaped (Γandl) groynes. In order to conduct the research, L-shaped groynes were installed in laboratory channel and three – dimensional components of flow velocity were measured by Acoustic Doppler velocimeter (ADV). According to the conducted research on turbulence intensity in longitudinal, transverse and deep directions and drawing the corresponding figures, it was determined that location of maximum turbulence intensity is in the vicinity of groynes wing and along the shear layer of flow. In addition, the values of maximum turbulence intensity in transverse and deep directions in Γ groyne are respectively 79.9 and 27.4 percent of maximum longitudinal turbulence intensity and in l groyne are respectively 67.9 and 23 percent of maximum longitudinal turbulence intensity. According to the conducted experiments in the present research, turbulent burst event was studied in various L- shaped groynes. In the cape zone of groynes, the probability of ejection is more than that of other quadruple events of turbulence. In upstream zones of groynes, the probability of occurrence of sweep is more than inward and outward internation. The probability of occurrence of sweep is decreased by approaching the groyne structure and again increases in the downstream of groyne.

***Keywords-*** *Turbulence Burst, Groyne, L-Shaped, Ejection, Sweep, Turbulence Intensity*

## I. INTRODUCTION

Rivers banks are often affected by natural hydraulic forces that lead to deformation, destruction and erosion [9,14]. Coastal protection is very important to prevent the economic losses including the loss of agricultural lands and disturbance in transportation infrastructure [7].one of the indirect methods of coastal protection is using the groyn structure due to the simple structure and low cost of establishment [9, 13, 15, 19, 22]. The groyn is located on the banks of rivers in two submerged and non- submerge modes [15]. Flow field around the groyn is a complex event that includes flow separation and vortex turbulent flow [4, 21]. The evaluation of flow field around groyns can be effective in better analysis of undermining by water trend and sedimentation around the groyns. According to the conducted researches by researchers on non- submerged groyns of rotational zone in downstream of groyn, it is seen that the direction of movement is upward in upper levels of flow and the direction of movement of flow is downward in layers close to the bed [5, 10]. One of the first laboratory researches was conducted by Ahmad on the groins that indicated the unsteadiness of flow around the griyn [1].

Duan et al [6] studied three-dimensional turbulent flow field around direct groyn in a laboratory channel with a length of 12.8m and a width of 0.608. In this research, micro ADV velocimeter was used to measure the turbulence of flow. The results of study showed that Reynolds stresses and the highest instantaneous turbulent velocity occur along the bottom line. In addition, since sediment transfer near the bed is associated with turbulence burst, the expansion of the cavity of undermining by water depends on the ejection. Kang and Yeo [8] conducted experiments in a channel with a length of 40m, width of 2m, height of 0.8m and constant depth of flow on L- shaped groyn (with length of 5 different wings) using ADV and LSPIV velocimeters to analyze the properties of flow (flow velocity and flow separation zone). Results showed that the velocity has increased 1.5 times in the main channel. In addition, velocity changes are trivial along the horn of groyn and and froude number of flow doesn't influence flow separation line. Kuhnle and Alonso [11] measured the components of flow velocity in 3484 points around a trapezoidal submerged groyn in a laboratory study using ADV velocimeter. Results showed that there is a significant difference between flow lines in smooth bed state and sedimentary bed. Shear stresses of rough bed are greater than smooth bed. Kumar and Malike [12] studied the pattern of flow around T- shaped and direct (with angle of 45, 60 and 90° relative to flow direction) groyns in the conditions of smooth bed using ANSYS FLUENT software. Results showed that the shape of groyn influences the turbulence of flow in layers near the bed. Safarzadeh et al [16] studied three-dimensional turbulent flow around T- shaped groins in smooth

channel and a 15 percent contraction in the width of channel using ADV velocimeter. Their results showed that geometry of groin has a significant impact on the pattern of flow particularly near the bed. Radan and Vaghefi [15] experimentally and numerically studied the impact of submergence percent of T- shaped groin on the pattern of undermining by water and flow pattern in rectangular channel with curvature of 90°, width of 0.6m,discharge of 25 L/S and 3 percent of submergence (0, 15, 25). Results showed that in submergence percent of 25, the changes of separation zone have a steep slope. Vaghefi et al [21] experimentally studied the flow field around a single T- shaped groyn in the arc of 90° using ADV velocimeter. Results showed that the pattern of flow is different along the arc and horizontal counterclockwise vortices are seen in upstream and downstream of groyns flow near the external wall. Asadzadeh et al [3] studied the structure of flow around the groyn with sloped wall of 75° in an experimental direct channel with solid bed using ADV velocimeter. Results showed that rest zone is generated by decreasing flow velocity behind the groyn and flow velocity is increased in the middle zones. Therefore, flow is divided into two upward and downward parts that leads to the establishment of horseshoe vortices. The highest value of stress component $-\overline{\acute{p}\acute{u}\acute{v}}$ occurs along the shear layer. In other conducted researches by Alizadeh Armaki et al [2] on the flow pattern around the groyn, it was noted that the present of flow separation plane in front of the groyn and in narrow section of the channel causes that a part of the flow acts as upward and other part as downward [2].

According to the conducted studies, so far, no comprehensive study has been conducted on the laboratory evaluation of turbulence intensity in longitudinal, transverse and deep directions and turbulence burst event around various L- shaped groynes to understand hydraulic flow around groynes. The purpose of present research is to measure three-dimensional components of flow velocity using ADV advanced three- dimensional velocimeter.

## II. MATERIALS AND EXPERIMENTS

The experiments of present research were conducted by a laboratory channel in hydraulic laboratory of agriculture and natural resources university of Khuzestan's Ramin with glassy walls and steel shields with 7 meter length and 0.5 meter width. Fig. 1 shows a view of the channel and equipment of the experiment. The groyns used in this research (Γ- and ٦- shaped) were made of Plexiglas rectangular plants of 1 cm thickness. The length of web and wing of groyn were 10 and 5 cm respectively (Fig. 2). The depth of flow was constant throughout the experiments that were 15 centimeters and end valve was used to control it. In addition, discharge was constant in all experiments that was 30 liter per second. Magnetic flow meter was used to measure flow rate. In all experiments, flow regime was subcritical and completely turbulent.

Figure 1. A view of channel position

Figure 2. Geometry of groynes

Vectrino three – dimensional velocimeter was used to measure three – dimensional components of flow velocity that is a new sample of ADV velocimeters that was made by Nortek company, Norway. Fig (3) shows ADV velocimeter during the pickup of velocity components in the laboratory channel attached to a moving device for ease of displacement and constant holding.

Figure 3. ADV velocimeter during the pickup of velocity components of flow

Measurement meshing of flow velocity is fine in non-uniform channel and near the groyn. It includes 20 transverse section and 7 altitude levels. There are 9 points in any transverse axis. Generally, 1260points have been measured for every groyn. Fig. 4 and Fig. 5 shows channel meshing in longitudinal and height directions. According to the conducted studies, 25 Hz frequency and the time of 3 min were determined for measuring every sample in this experiment. According to the determined frequency and time at point of 4500 data, velocity was measured by ADV velocimeter in 3 directions and was recorded by vectrino software. Then, the corresponding graphs were drawn by changing the format of data and using Excel and single plot softwares. According to the fact that the components of instantaneous velocity are obtained in three directions by ADV velocimeter, average velocities (U, V, W), oscillating velocity ( $\acute{u}_i, \acute{v}_i, w_i$) and turbulence parameters of flow can be calculated by using these instantaneous velocities ($u_i, v_i, w_i$) at a specified point in the turbulence flow field. Oscillating velocities are obtained by following equations.

$$u_i' = u_i - U \quad (1)$$

$$v_i' = v_i - V \quad (2)$$

$$w_i' = w_i - W \quad (3)$$

Turbulence intensities of flow in longitudinal, vertical and transverse directions and turbulent kinetic energy are expressed as $\sqrt{\overline{u'^2}}$, $\sqrt{\overline{v'^2}}$, $\sqrt{\overline{w'^2}}$ and TKE [16, 20]. These turbulence intensities are obtained as root mean square:

$$u'_{RMS} = u^+ = \left[\frac{1}{n}\sum_{i=1}^{n}(u_i - U)^2\right]^{0.5} \quad (4)$$

$$v'_{RMS} = v^+ = \left[\frac{1}{n}\sum_{i=1}^{n}(v_i - V)^2\right]^{0.5} \quad (5)$$

$$w'_{RMS} = w^+ = \left[\frac{1}{n}\sum_{i=1}^{n}(w_i - W)^2\right]^{0.5} \quad (6)$$

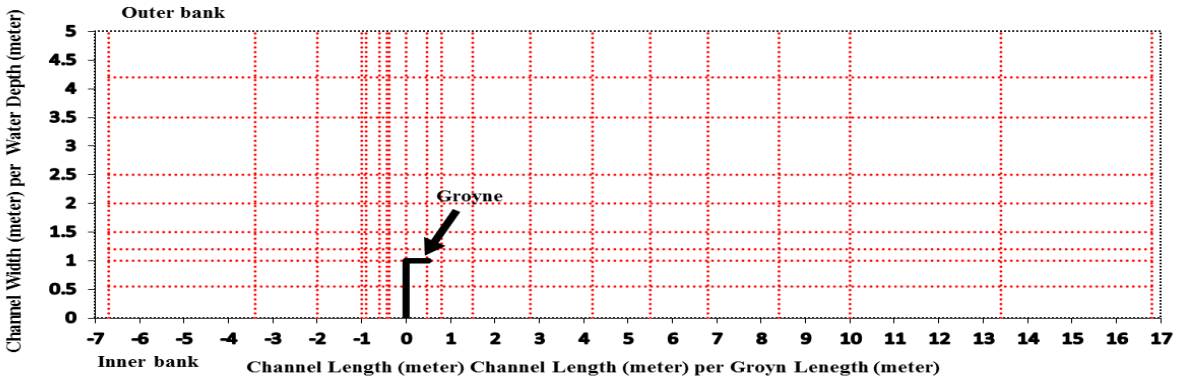


Figure 4. Meshing the points of pickup velocity components in horizontal plane

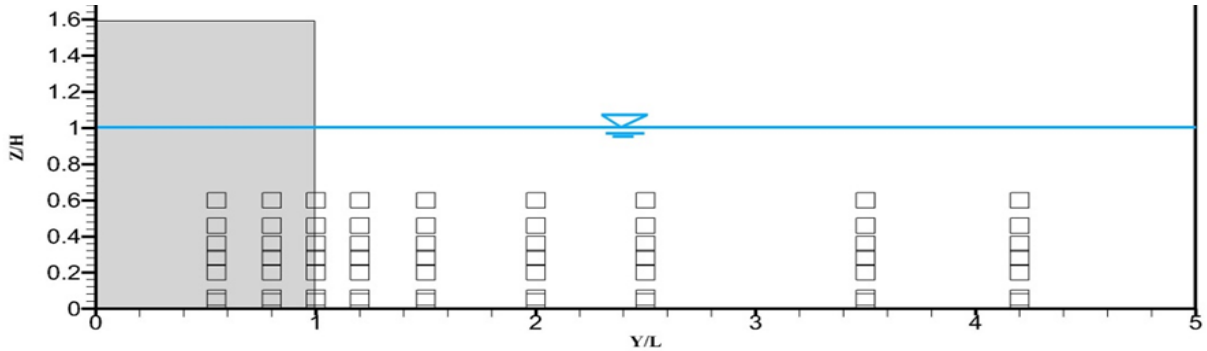


Figure 5. Meshing the points of pickup velocity components in vertical plane in transverse section

## III. DISCUSSION

Figs. 6 - 8 shows flow patterns around the studied groyns based on the mean time values of the measured velocity series at each point in two altitudes of 0.6 and 9 cm from the floor and in distance 7 and 17 times the length of groyn's web in the upstream and downstream of the groyns. Generally, in two levels of depth in the upstream areas of the groyns, the flow lines are relatively parallel and gradually diverge from the lnner bank to the middle areas of the channel due to the contact

with groyn (contraction section of channel) which increases the flow velocity in this area of the channel. According to Figs. 6 and 7, the width of flow separation zone is decreased and the extent of the formed vortex is increased at downstream by increasing altitude level. In addition, the center of the formed vortex at downstream is generated in closer distance from ⅂ groyn. In ⅂ - shaped groyn in altitude level of 0.6 cm after the contact of flow with the groyn, flow in upstream of the groyn is in the opposite direction and diverges to the middle areas (Fig. 7). The width of flow separation zone in this groyn and in 0.6cm level from the floor is greater than that of Γ groyn. However, at higher altitude levels, the width of flow separation zone has decreased, but downstream planes influence the flow of upstream zones. According to 20 percent, contraction limit of channel, the flow crashes with the outer bank of the channel and diverts to the middle zones (Fig. 8).

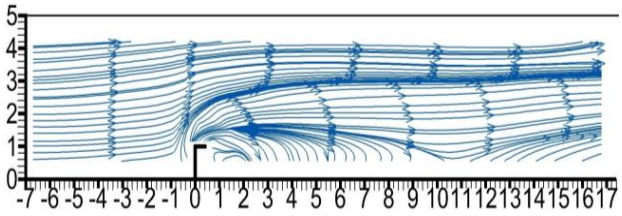

Figure 6. The comparison of flow lines around the groyn at the level of 4 percent of flow depth from the bed in Γ - shaped groyn

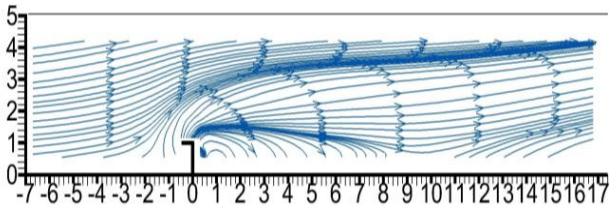

Figure 7. The comparison of flow lines around the groyn at the level of 4 percent of flow depth from the bed in ⅂ - shaped groyn

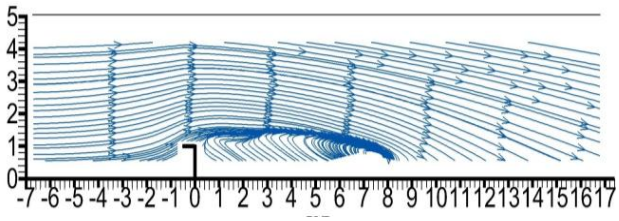

Figure 8. The comparison of flow lines around the groyn at the level of 60 percent of flow depth from the bed in ⅂ - shaped groyn

### *A. Longitudinal components of the velocity*

Figs. 9 - 12 show the samples of the contours of dimensionless longitudinal component of the flow velocity at two depth levels of 4 and 60 percent from the floor. According to the figure at both altitude levels and at each groyn, flow velocity in front of the groyn is higher than other zones due to the decrease of channel's width along shear layer of the flow. In addition, velocity is increased by increasing altitude level of dimensionless longitudinal component.

According to Figs. 9 and 11, a zone is seen with low velocity at upstream of groyns that indicates the presence of reverse flow and the formation of horseshoe vortices in this zone, while the velocity increases in this zone at the level close to the surface of flow (Figs. 10 and 12). According to this figure, the intensity of reverse flow at upstream of ⅂ - shaped groyn is higher than that of Γ groyn.

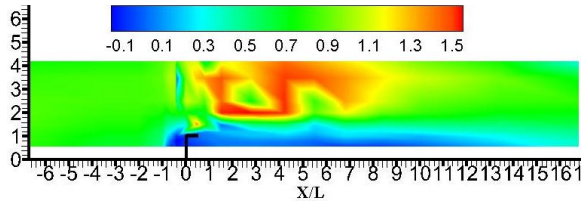


Figure 9. The magnitude of longitudinal component of flow velocity at level of 4 percent of flow depth from the floor in Γ - shaped groyn

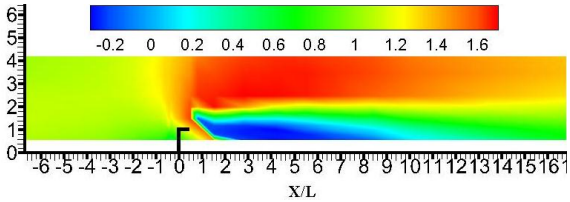


Figure 10. The magnitude of longitudinal component of flow velocity at level of 60 percent of flow depth from the floor in Γ- shaped groyn

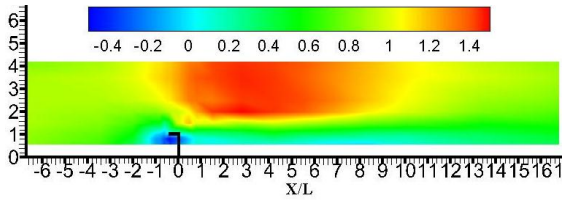


Figure 11. The magnitude of longitudinal component of flow velocity at level of 4 percent flow depth from the floor in ⅂- shaped groyn

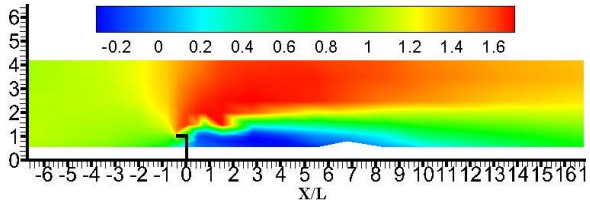


Figure 12. The magnitude of longitudinal component of flow velocity at level of 60 percent of flow depth from the floor in ⅂- shaped groyn

### B. *Vertical component of flow velocity*

Contours of vertical component of velocity at levels of 4 and 60 percent of flow depth from the floor are shown in Figs. 13 and 14. As it is shown, flow velocity has decreased in front of the groyn. Maximum velocity has formed in downward direction in vicinity of groyn's wing at level close to the bed, while at a level close to the surface the flow of the zone is formed with a negative velocity, which is slightly less in the zone between the wing and web of the groyn. In addition, 3 zones are seen with a relatively maximum upward velocity in front of the l-shaped groyn and in central zone of the channel.

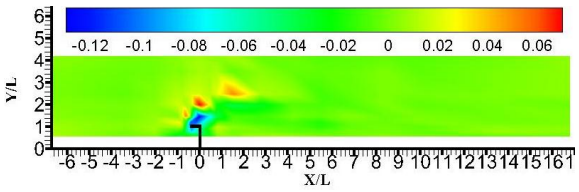


Figure 13. The magnitude of vertical component of the velocity at level of 4-percent of flow depth from the floor in l-shaped groyn

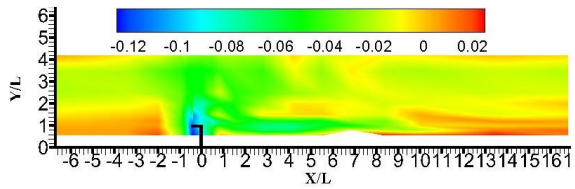


Figure 14. The magnitude of vertical component of the velocity at level of 60 percent of flow depth from the floor in ⅂ - shaped groyn

### C. *Turbulence intensity in longitudinal, transverse and deep directions*

Figs. 15 and 16 show the distribution of turbulent kinetic energy at 4 and 60 percent levels of flow depth from the floor in ⅂ - shaped groyn. According to this figure, the maximum of turbulent kinetic energy is formed along shear layer of the flow and the level close to the flow surface. In addition, a turbulent zone is formed in the cape of groyn at the level close to the bed. This zone starts from upstream of the groyn and extends at an angle of about 60° along the flow separation layer to the front of the groyn. The formation of this turbulent zone is attributed to the formation of horseshoe vortices in the cape of groyn. Also the expansion and strain of TKE are consistent with flow separation plane and its intensity is higher in l-shaped groyn. In addition, the distribution of kinetic energy in upper layer is higher than that of the layer close to the floor due to the high velocity of flow in upper layer relative to the layers close to the bed.

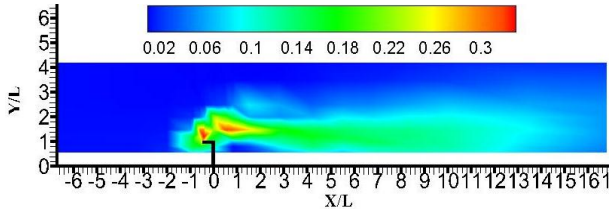


Figure 15. Distribution of turbulence intensity of the flow in 4 percent level of flow depth from the bed in ⅂ - shaped groyn

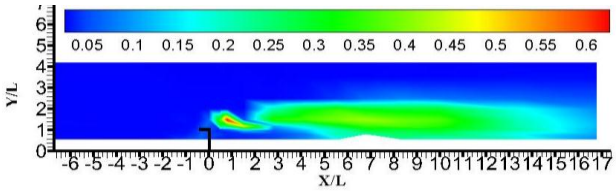


Figure 16. Distribution of turbulence intensity of the flow in 60 percent level of flow depth from the bed in ⅂ - shaped groyn

According to the importance of study of flow turbulence in the layers close to the bed in open channels due to the generation of maximum shear stress and bed undermining by water discussion, Figs. 17 - 22 shows the values of turbulence intensity of $u^+$, $v^+$, and $w^+$ at 4 percent level of flow depth from the bed. As it is seen, the place of occurrence of maximum turbulence is in vicinity of groyn*'s* wing and along shear layer of the flow in three longitudinal, transverse and deep directions. In addition, the highest value of flow turbulence is in longitudinal direction and the lowest value of it is in deep direction of the flow. In order to better comparison of maximum values of flow turbulence intensity in different directions, maximum values of $u^+$, $v^+$ and $w^+$ along the channel are presented in Table. 1. In addition, the values of maximum turbulence intensity in transverse and deep directions in Γ griyn are respectively 79.9 and 27.4 of maximum longitudinal turbulence intensity and in ⅂ gryin are respectively 67.9 and 23 of maximum longitudinal turbulence intensity.

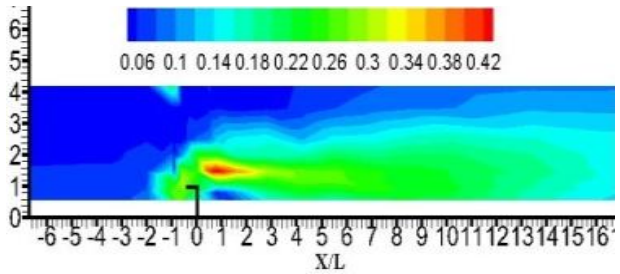


Figure 17. Distribution of flow turbulence intensities in a depth equivalent to 4 percent of flow depth from the bed in longitudinal directions ($u^+$) in ⅂ - shaped groyn

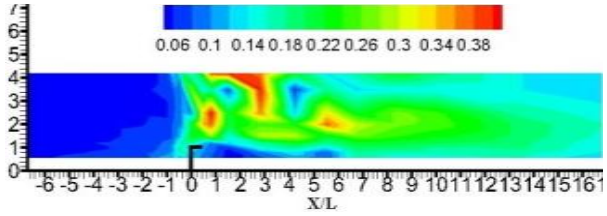


Figure 18. Distribution of flow turbulence intensities in a depth equivalent to 4 percent of flow depth from the bed in longitudinal directions ($u^+$) in Γ- shaped groyn

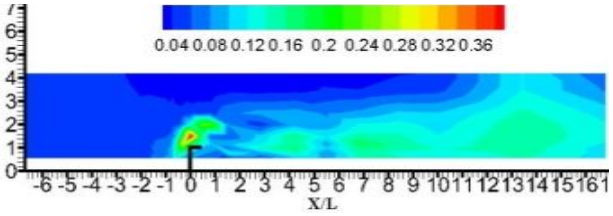


Figure 19. Distribution of flow turbulence intensities in a depth equivalent to 4 percent of flow depth from the bed in transverse directions ($v^+$) in Γ- shaped groyn

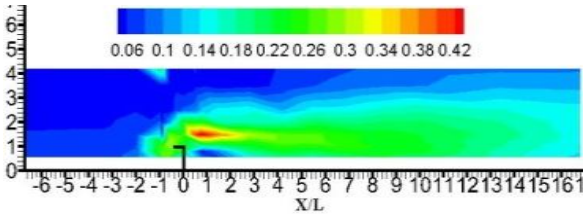


Figure 20. Distribution of flow turbulence intensities in a depth equivalent to 4 percent of flow depth from the bed in transverse directions ($v^+$) in ٦ - shaped groyn

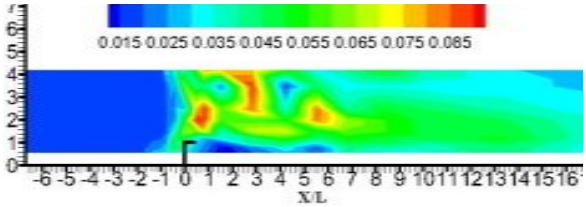


Figure 21. Distribution of flow turbulence intensities in a depth equivalent to 4 percent of flow depth from the bed in deep directions ($w^+$) in Γ- shaped groyn

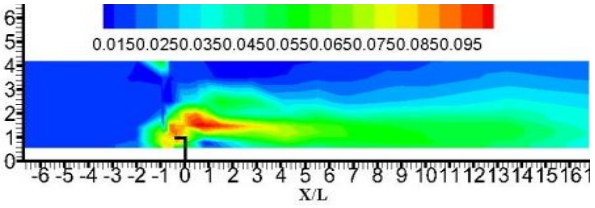


Figure 22. Distribution of flow turbulence intensities in a depth equivalent to 4 percent of flow depth from the bed in deep directions ($w^+$) in ٦ - shaped groyn

TABLE I. THE COMPARISON OF MAXIMUM TURBULENCE INTENSITIES IN LONGITUDINAL, TRANSVERSE AND DEEP DIRECTIONS IN L- SHAPED GROYN LE TYPE STYLES

| Groyn | Turbulence Intensities | | |
|---|---|---|---|
| | u+(m/s) | v+(m/s) | w+(m/s) |
| Γ- Shaped Groyn | 0.44 | 0.39 | 0.1 |
| ٦- Shaped Groyn | 0.41 | 0.4 | 0.09 |

### *D. Turbulent burst event*

Fluid bundles near the bed are separated from near bed levels and transported to upper levels due to the undulate surfaces of near- bed flow that such a process is called turbulent burst event. In order to hold continuity equation, high velocity bundles of fluid are transferred from upper levels to lower levels that such a process is called sweep. In addition, the transfer of low velocity bundles of fluid from near- bed levels to upper levels is called ejection. According to the displacement of fluid bundles, the sign of components of fluctuations of longitudinal and deep velocity can be different. If both components of surface and deep fluctuations of velocity have positive sign, outward internation will occur and if both components of velocity have negative sign, inward internation will occur. The sum of these four events forms turbulent burst process. The study f turbulence events are important to detect areas prone to undermining by water and sedimentation [19]. According to Fig. 23 in zone (I), outward internation is seen. In zone (II), ejection is seen. Zone (III) is related to inward internation. In zone (IV), sweep event is seen. Zone V (Hole) is related to the events that have trivial power and don't influence transport process of sedimentation.

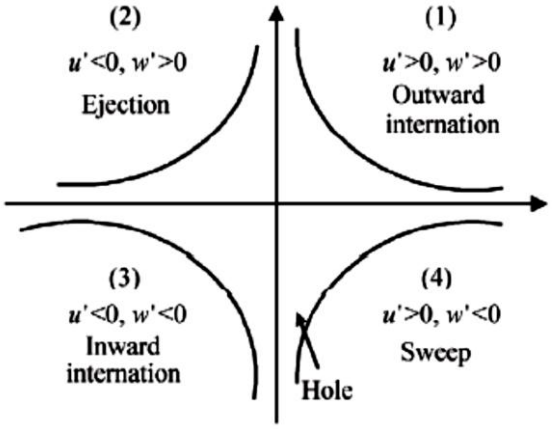


Figure 23. Division of zones for studying turbulent burst event

Equation (5) is used to determine these zones [6].

$$X_Q = \begin{cases} 1 \; if \; |u_i' w_j'| \geq H . \sqrt{\overline{u_i'^2}} . \sqrt{\overline{w'^2}} \\ 0 \; if \; |u_i' w'| < H . \sqrt{\overline{u_i'^2}} . \sqrt{\overline{w'^2}} \end{cases} \quad (5)$$

In above equation, $\acute{u}_\iota$ is the fluctuations of surface components of velocity and $\acute{w}$ is the fluctuations of deep component of the velocity. If $X_Q$=1, corresponding event is used in analysis and if $X_Q$=0, corresponding event is weak and is disregarded. The high value of H parameter indicates that corresponding event is strong in analyses. According to the study of Bee et al (2004), H=2 is set. The probability of occurrence of each of the quadruple events is each zone is defined as follows.

$$P_i = \frac{n_i}{\sum_{i=1}^{4} n_i} \quad (6)$$

In above equation, $P_i$ is the probability of occurrence of each of the turbulent burst events and $n_i$ is the number of each of the eventsl. Fig. 24 and 25 shows the changes of probability of generating turbulence events along the channel and at a distance of 16% the channel width from the lnner bank in each of the studied groyns. According to this figure, the probability of ejection is higher than other events in cape zone of the groyn. In addition, the probability of occurrence of sweep event is higher than inward and outward internations in upstream zones of the groyns. The probability of its occurrence is decreased by approaching groyn structure and again increases in downstream of the groyn.

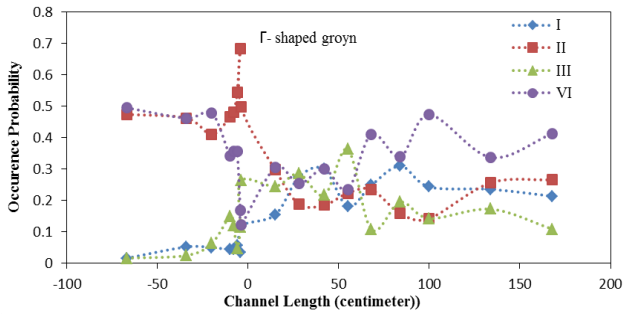


Figure 24. The changes of probability of generating quadruple events near the floor along the channel of Γ- shaped groyn

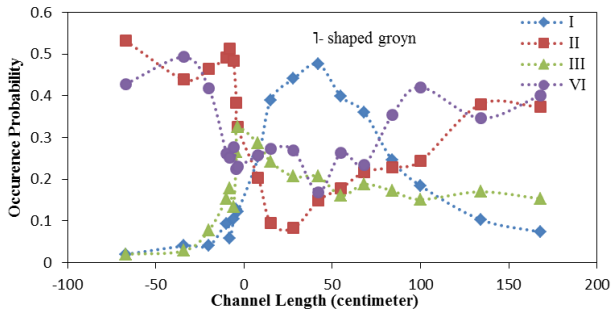


Figure 25. The changes of probability of generating quadruple events near the floor along the channel of ך- shaped groyn

## IV. CONCLUSION

Present research studied the structure of three- dimensional and turbulent flow around a variety of ך- and Γ- shaped groyns in a direct channel with solid bed. The study of flow lines in upstream and downstream of the groyns at 4 and 60 percent levels from the floor showed that at contraction section of the channel, the curvature of flow is from the lnner bank of the channel toward central zone of the flow and is higher at near the bed level in ך- shaped groyn than Γ- shaped groyn. The conducted studies show that formed vortex in downstream of the structure is further developed in upstream of the flow. In addition, the expansion of this vortex is increased in transverse direction. The maximum of vertical velocity component of the flow occurs in downstream of groyns cape. Its intensity in Γ groyn is higher than ך groyn. The highest value of flow turbulence is in longitudinal direction and its lowest value is related to deep direction of the flow. The values of maximum turbulence intensity in transverse and deep directions in Γ griyn are respectively 79.9 and 24.7 of maximum longitudinal turbulence intensity and in ך gryin are respectively 67.9 and 23 of maximum longitudinal turbulence intensity. The expansion and strain of TKE are consistent with flow separation plane and its intensity is higher in ך- shaped groyn. In cape zone of groyns, the probability of ejection is higher than other quadruple events of turbulence. In addition, the probability of occurrence of sweep event is higher than inward and outward internations in upstream zones of the groyns. The probability of its occurrence is decreased by approaching groyn structure and again increases in downstream of the groyn.


## ACKNOWLEDGEMENT

This work is supported by the Ramin Agriculture and Natural Resources University of Khuzestan, Iran.


## REFERENCES


[1] M. Ahmed, " Experiments on Design and Behavior of Spur-Dikes," In proc. Minnesota International Hydraulics Convention, Minneapolis. 59-145, 1953.

[2] H. Alizadeh Armaki, M. Vaghefi, M. Ghodsian, and M, Khosravi, (2015). "Experimental Investigation of Flow and Scour Pattern around Submerged Attracting and Repelling T head Spur Dike,". Modares Civil Engineering Journal (MCEL), 15. (In Persian)

[3] F. Asadzadeh, A. Safarzadeh, and S. A. A. Salehi Neyshabouri, (2016). "Experimental study of flow around a spur dike with side slope". Modares Civil Engineering Journal (M.C.E.J). 16(1). (In Persian)

[4] A. A. Dehghani, M. Barzali, R. Fazloula, and M. KH. Zea Tabar Ahmadi, (2009). "Experimental Study of Scouring around a Series of L-head Groynes". Journal of Water and Soil Conservalion. 16(3). (In Persian)

[5] J. G. Duan, (2009). "Mean flow and turbulence around a laboratory spur dike". Journal of Hydraulic Engineering, 135(10), 803–811.

[6] J. Duan, L. He, G. Wang, and X. Fu (2011). "Turbulent Burst around Experimental Spur Dike". International Journal of Sediment Research, 26(4): 471-486.

[7] 7. M. Hemmati, M. Ghomeshi, H. Ahmadi, and S. Lanzoni, ( 2016). "Scour depth around flat and sloped crest bendway weirs: a laboratory study". International Journal of River Basin Management, 14(1): 83-93.

[8] J. Kang, and H. Yeo, (2011). "Experimental Study on the Flow Characteristics of¬-Type Groyne". Engineering, 3(10), 1002.

[9] H. Karami, H. Basser, A. Ardeshir, and S. H. Hosseini, (2014). "Verification of numerical study of scour around spur dikes using experimental data". Water and Environment Journal, 28(1): 124-134.

[10] M. Koken, and G. Constantinescu,(2008). An investigation of the flow and scour mechanisms around isolated spur dikes in a shallow open channel: 1. Conditions corresponding to the initiation of the erosion and deposition process. Water Resources Research, 44(8).

[11] R. Kuhnle, and C. Alonso, (2013). "Flow near a model spur dike with a fixed scoured bed". International Journal of Sediment Research, 28(3), 349-357.

[12] M. Kumar, and A. Malik, ( 2016). "3D Simulation of Flow around Different Types of Groyne Using ANSYS Fluent". Imperial Journal of Interdisciplinary Research, 2(10).

[13] M.Mehraein, M. Ghodsian, M. K. Mashizi, and M. Vaghefi,(2017). "Experimental Study on Flow Pattern and Scour Hole Dimensions Around a T-Shaped Spur Dike in a Channel Bend Under Emerged and Submerged Conditions". International Journal of Civil Engineering, 1-16.

[14] S. Pagliara, and S. M. Kurdistani, ( 2017). "Flume experiments on scour downstream of wood stream restoration structures". Geomorphology, 279, 141-149.

[15] P. Radan, and M. Vaghefi, ( 2016). "Flow and scour pattern around submerged and non-submerged T-shaped spur dikes in a 90° bend using the SSIIM model". International Journal of River Basin Management, 14(2): 219-232.

[16] A. Safarzadeh, S. A. A. Salehi Neyshabouri and A. R. Zarrati, (2016). "Experimental Investigation on 3D Turbulent Flow around Straight and T-Shaped Groynes in a Flat Bed Channel". Journal of Hydraulic Engineering, 04016021.

[17] A. N. Sukhodolov, T. A. Sukhodolova, and J. Krick, ( 2016). "Effects of vegetation on turbulent flow structure in groyne fields". Journal of Hydraulic Research, 55(1): 1-15.

[18] S. Tofighi, J. M. Vali Samani, and S. A. Ayyoubzadeh, ( 2016). "Bursting Events in Pressure Flushing with Expanding Bottom Outlet Channel within Dam Reservoir". Journal of Water and Soil. Vol. 30, No. 5, 1358-1369. (In Persian)

[19] W.S. Uijttewaal, ( 2005). "Effects of groyne layout on the flow in groyne fields: Laboratory experiments". Journal of Hydraulic Engineering, 131(9), 782-791.

[20] M. Vaghefi, and M. Akbari, ( 2015). "Determining Turbulence Intensity in a 180 Degree Sharp Bend Channel Using Experimental Data".

[21] M. Vaghefi, M. Ghodsian, and M. Akbari, (2017). "Experimental Investigation on 3D Flow around a Single T-Shaped Spur Dike in a Bend". Periodica Polytechnica Civil Engineering.

[22] Y. Wang, F. Jin, F, C. Zhang, J. Wang, Y. Hu, and J. Wang, (2017). "Novel method for groyne erosion stability evaluation". Marine Georesources & Geotechnology, 1-20.